Modelling head injury due to unmanned aircraft systems collision: Crash dummy vs human body

Borrdephong Rattanagraikanakorn , Michiel Schuurman , Derek I. Gransden , Riender Happee , Christophe De Wagter , Alexei Sharpanskykh & Henk A.P Blom

Published online: 24 Aug 2020.

Submit your article to this journal ↗

Article views: 264

View related articles ↗

View Crossmark data ↗

Taylor & Francis
Taylor & Francis Group

Modelling head injury due to unmanned aircraft systems collision: Crash dummy vs human body

Borrdephong Rattanagraikanakorn[a] , Michiel Schuurman[b], Derek I. Gransden[c], Riender Happee[d] , Christophe De Wagter[e], Alexei Sharpanskykh[f] and Henk A.P Blom[g]

[a]Aerospace Structures & Materials Department, Faculty of Aerospace Engineering, Delft University of Technology, Delft The Netherlands; [b]Aerospace Structures & Materials Department, Faculty of Aerospace Engineering, Delft University of Technology, Delft, The Netherlands; [c]Bharti School of Engineering, Laurentian University, Sudbury, Canada; [d]Cognitive Robotics, Mechanical Engineering, Delft University of Technology, Delft, The Netherlands; [e]MavLab, Faculty of Aerospace Engineering, Delft University of Technology, Delft, The Netherlands; [f]Section Air Transport and Operation, Faculty of Aerospace Engineering, Delft University of Technology, Delft, The Netherlands; [g]Section Air Transport and Operation, Faculty of Aerospace Engineering, Delft University of Technology, Delft, The Netherlands

ABSTRACT

Recent developments in the concept of UAS operations in urban areas have led to risk concerns of UAS collision with human. To better understand this risk, head and neck injuries due to UAS collisions have been investigated by different research teams using crash dummies. Because of the limitations in biofidelity of a crash dummy, head injury level for a crash dummy impact may differ from the human body impact. Therefore, the aim of this paper is to investigate differences in head and neck injuries subject to UAS collision between an often-used Hybrid III crash dummy and a human body. To perform such investigation, multibody system (MBS) impact models have been used to simulate UAS impacts on validated models of the Hybrid III crash dummy and the human body at various impact conditions. The findings show that the Hybrid III predicts similar head and neck injury compared to the human body when UAS collides horizontally from front and rear. However, the Hybrid III over-predicts head injury due to horizontal side impact. Moreover, under vertical drop and 45 degree elevated impact of UAS, the Hybrid III under-predicts head injury, and over-predicts neck injury.

1. Introduction

Unmanned aircraft systems (UAS) are expected to operate in low-level airspace in an urban environment where population density is high. The risk from such implementation has given rise to the question of the safety of people on the ground. This motivates efforts to understand the impact severity of UAS collision on human through analytical or experimental approaches. In impact experiments, an anthropomorphic test device (ATD), i.e. the Hybrid III crash dummy, is widely used as a representative substitution of a real human body. Campolettano [1] performed a series of live flight test and impact drop test using three different UAS weight classes on an instrumented Hybrid III. The Alliance of System Safety of UAS through Research Excellence (ASSURE) research group also conducted a series of controlled impact drop test using DJI Phantom III UAS on the Hybrid III crash dummy at various UAS impact attitudes and speeds [2–4]. These tests provide valuable insights into head and neck injury from UAS collision. The aim of the test was to estimate the range of head injury risks to humans due to UAS impact.

Even though Hybrid III is based on the human body, for road accidents it has been shown that limitations in biofidelity of a crash dummy can result in different biomechanical head and neck responses compared to the real human [5]. The human body neck complex is the spine which is a biomechanical structure composed of bony vertebrae, ligaments, and intervertebral discs [6]. It is a flexible structure with a primary function to protect the spinal cord and nerve roots while carrying loads and perform the physical motion. The Hybrid III neck is designed to represent the cervical human spine by connecting the head and torso through a rigid attachment. The neck itself is a one-piece column made of rubber separated by aluminium discs and there is no inherent curvature to the Hybrid III neck column [6].

Based on experimental work by Sances [7], a comparison of inverted drops on the Hybrid III and human cadavers showed that the dummy neck was two to four times stiffer than human cadavers. Additionally, an experiment by Sances [8] indicated that the Hybrid III crash dummy transmits about 70-75% of the applied force from the head or upper neck to the lower neck area. On the other hand, only about 20-30% of the applied force was transmitted from the head to the lower neck in the study on a human cadaver. Such differences can

Table 1. Summary of injury level results from Section 3 for Hybrid III dummy relative to human body.

			Injury of Hybrid III relative to human body	
Impact Case	θ (Impact Elevation)	Ψ (Impact Direction)	Head Injury	Neck Injury
1	0° (Horizontal)	0° (Frontal)	Similar	Similar
2		90° (Side)	Higher	Similar
3		180° (Rear)	Similar	Similar
4	45° (Elevated)	0° (Frontal)	Lower	Higher
5		90° (Side)	Lower	Higher
6		180° (Rear)	Lower	Higher
7	90° (Vertical Drop)	0° (Frontal)	Lower	Higher
8		90° (Side)	Lower	Higher
9		180° (Rear)	Lower	Higher

Figure 1. DJI Phantom III UAS used in impact modelling: (a) real-world system and (b) multibody system (MBS) model developed in MADYMO[11]. The two landing skids are neglected in the MBS model since they are such flexible that their impact effect is negligible [11].

lead to a discrepancy in head injury level on a human body and a Hybrid III crash dummy used in testing.

In any investigation to determine the impact severity of a particular vehicle, it is vital that the measuring instrument is appropriate to serve the investigation objective. In this case, it is important to know whether a Hybrid III dummy is a suitable measuring instrument for an investigation on UAS collision severity and can realistically represent a human body. If the discrepancy between the Hybrid III dummy and a real human body is significant, then it is important to address the scale of such difference. Therefore, the primary aim of this paper is to investigate differences in head and neck injury levels on a Hybrid III dummy and on a human body due to UAS collisions by using validated Multi-body system (MBS) models of the Hybrid III dummy, human body, and UAS.

This paper is organized as follows. Section 2 describes the modelling and analysis methods including the models used in the simulation. Section 3 presents the comparative results from the models developed and simulated in MADYMO. Sections 4 and 5 present the discussion of the results and the conclusion, respectively.

The current paper forms a significantly extended version of the paper presented at the 2019 AIAA Aviation Forum conference [9].

2. Modelling and simulation approach

2.1. UAS, hybrid III and human body models

For a comparison of injuries due to UAS collision with a Hybrid III crash dummy versus a human body, validated numerical simulation models are implemented in the software package called MADYMO [10] and are subsequently utilized. The UAS chosen for this study was the DJI Phantom III with a take-off weight (W_0) of 1.28 kg. For this specific UAS, a multibody system (MBS) model shown in Figure 1 has been developed and validated in previous research [11]. For the validation, the simulation results obtained from this MBS model of a DJI Phantom III colliding with a Hybrid IIII dummy have been compared to the crash test data obtained by the ASSURE research group [4]. Impact data from the ASSURE research group was chosen for validation of this impact model because of its large range of controlled impact cases and precise measuring data.

To simulate injury levels within MADYMO, the UAS MBS model that was previously coupled with a 50th percentile MBS model of a Hybrid III dummy is now also coupled with a 50th percentile MBS model of a human body, as shown in Figure 2. '50th percentile' refers to the size of the human body which is equivalent to the average North American male. An MBS model of this 50th percentile Hybrid III has been validated against a real Hybrid III at various load conditions [12,13] which is distributed with MADYMO (filename: d_hyb350el_Q, version 2.0). A 50th percentile model of a human body is also distributed with MADYMO (filename: h_occ50fc, version 5.2) and was originally published by Happee [14,15]. This human body model is also an MBS with a passive muscle model and the skin is modelled using a facet surface which is a mesh of shell-type massless contact elements. The skeleton of this human body model consists of chains of rigid bodies connected by kinematic joints. The biomechanical data including joint characteristics and mechanical properties are based on biomechanical data and are validated using volunteer and post mortem human subject (PMHS) [16].
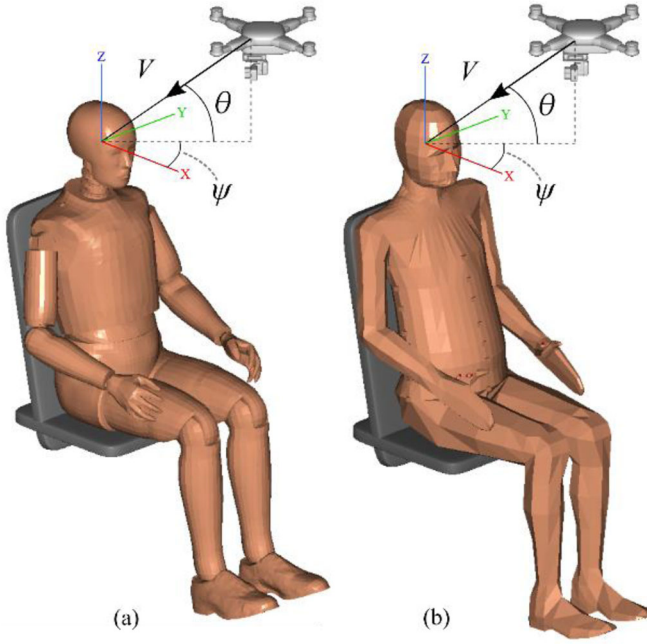
Figure 2. Simulation setup in MADYMO of UAS collisions on (a) the Hybrid III model and (b) the human body model.

2.2. Simulation setup

Because the head is the most vulnerable part of the human body, this paper focuses on MBS simulation of impact of DJI Phantom III collision with the head of the Hybrid III dummy versus the head of the human body. In the simulation set up, the Hybrid III dummy and the human body are seated on non-smooth rigid seats with full back support. The velocity vector of the UAS is aligned with the head centre of gravity (CG) of the Hybrid III and the human body. The UAS angle of attack was fixed at 0° from the horizontal axis for all impact case.

Impact simulations were performed by varying three main parameters; impact velocity (V), impact elevation (θ), and impact direction (ψ) (see Figure 2). Impact velocity (V) is varied from 0 to 18 m/s with an increment of 2 m/s. Note that impact velocity is converted and presented in a form of impact energy, varying from 0 to 196 J which is equivalent to 0 to 18 m/s for the DJI Phantom III. Impact elevation (θ) is set to 0° (horizontal impact), 45° (elevated impact) and 90° (vertical drop). The horizontal and elevated impact cases represent a loss of control failure mode in which the UAS flies directly onto the head. The vertical drop case represents a failure mode in which a UAS falls to the ground due to the complete loss of power. Lastly, impact direction (ψ) is set to 0° (frontal), 90° (side), and 180° (rear). The simulation was run on a 2.6 GHz processor, resulting in computational time of approximately 60 s and 120 s for the human body and the Hybrid III dummy, respectively.

To assess the risk of serious head injuries such as traumatic brain injury or skull fracture, the head injury criterion (HIC) was used [17,18]. Functionally, the HIC represents the peak average power delivered to the head [19]. It measures the likelihood of head injury due to impact by integrating head CG acceleration over time, and the formula is,

$$HIC = \left\{ (t_2 - t_1) \left[\frac{1}{t_2 - t_1} \int_{t_1}^{t_2} a(t)\,dt \right]^{2.5} \right\}_{max} \quad (1)$$

Where a(t) is the head CG acceleration curve, t_1 is the initial impact time and t_2 is the final impact time. There are two time-range limits which are 15 ms and 36 ms. In this paper, the 15 ms time range limit is chosen as it is more appropriate for a short-duration impact study. The HIC with 15 ms time range limit is referred to as HIC_{15} which is the term used in the rest of the paper. Based on FMVSS and NCAP, the HIC value of 700 is considered to be a minimum safety standard where the probability for skull fracture ($AIS \geq 2$) for the mid-sized male is 31% [20]. To measure head acceleration, both the Hybrid III and the human body models are instrumented with 3 single-axis accelerometers positioned at the CG of the heads. A low-pass filter with a channel frequency class (CFC) 1000 is applied to linear acceleration curves from the head CG accelerometers.

Furthermore, the N_{ij} is a neck injury criterion that considers the upper neck force and moment proposed by the National Highway Traffic Safety Administration (NHTSA) [21]. The 'ij' represents indices for the 4 injury mechanisms; namely N_{TE}, N_{TF}, N_{CE} and N_{CF}. The first index j represents the actual load (Tension or Compression) while the second index j represent sagittal plane bending moment (neck Flexion or Extension). The current performance limit of the N_{ij} is 1 which represents a 22% risk of AIS level 3 [22]. The equation for the N_{ij} is:

$$N_{ij} = \left| \frac{F_{Z,i}}{F_{int,i}} \right| + \left| \frac{M_{Y,j}}{M_{int,j}} \right| \quad (2)$$

where $F_{z,i}$ is the upper neck force in Z-axis, $F_{int,i}$ is the threshold force, $M_{Y,j}$ is the upper neck moment about Y-axis and $M_{int,j}$ is the threshold moment.

## 3. Modelling results for hybrid III dummy vs. human body

3.1. UAS impact injuries

3.1.1. Overall kinematic of head/neck system
From the simulation, the overall kinematics of the head and neck of the Hybrid III and the human body is presented in Figures 3–5. The impact sequences shown in the figures captured the kinematic of the head and neck of the Hybrid III and the human body at every 6 ms starting from contact initiation between the UAS and the head. The comparison is done by comparing the trajectory and displacement of the CG of the Hybrid III and human body heads.

Firstly, Figure 3 shows the impact sequences for $\theta = 0°$ (horizontal impact) of UAS impacting the heads for ψ equal to 0°, 90° and 180° (corresponding to frontal, side, and rear impact, respectively). For $\psi = 0°$ (frontal impact), as shown in Figure 3(a), the Hybrid III head and neck complex can realistically mimic the movement of the human body head and neck with similar head translational and rotational
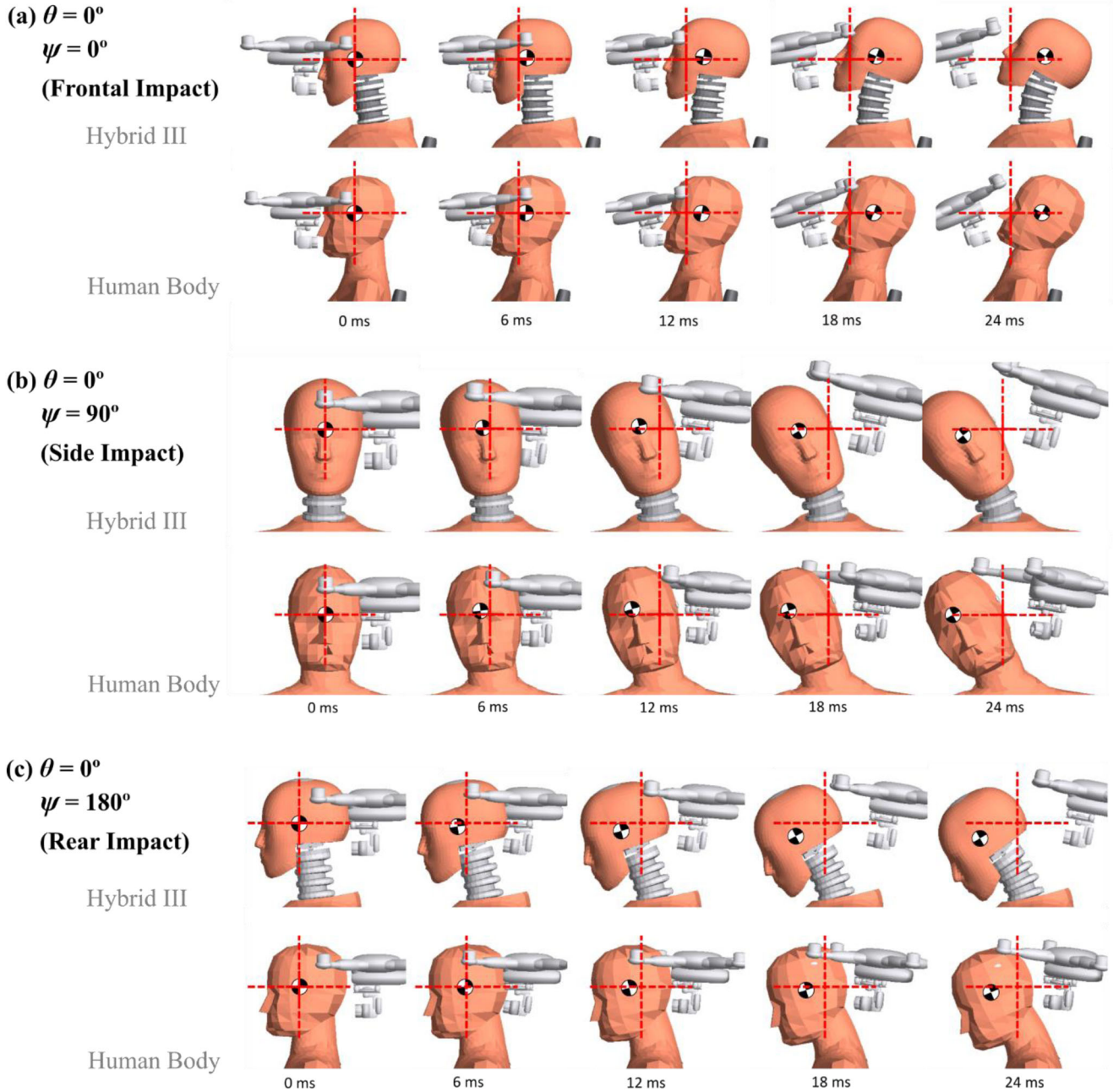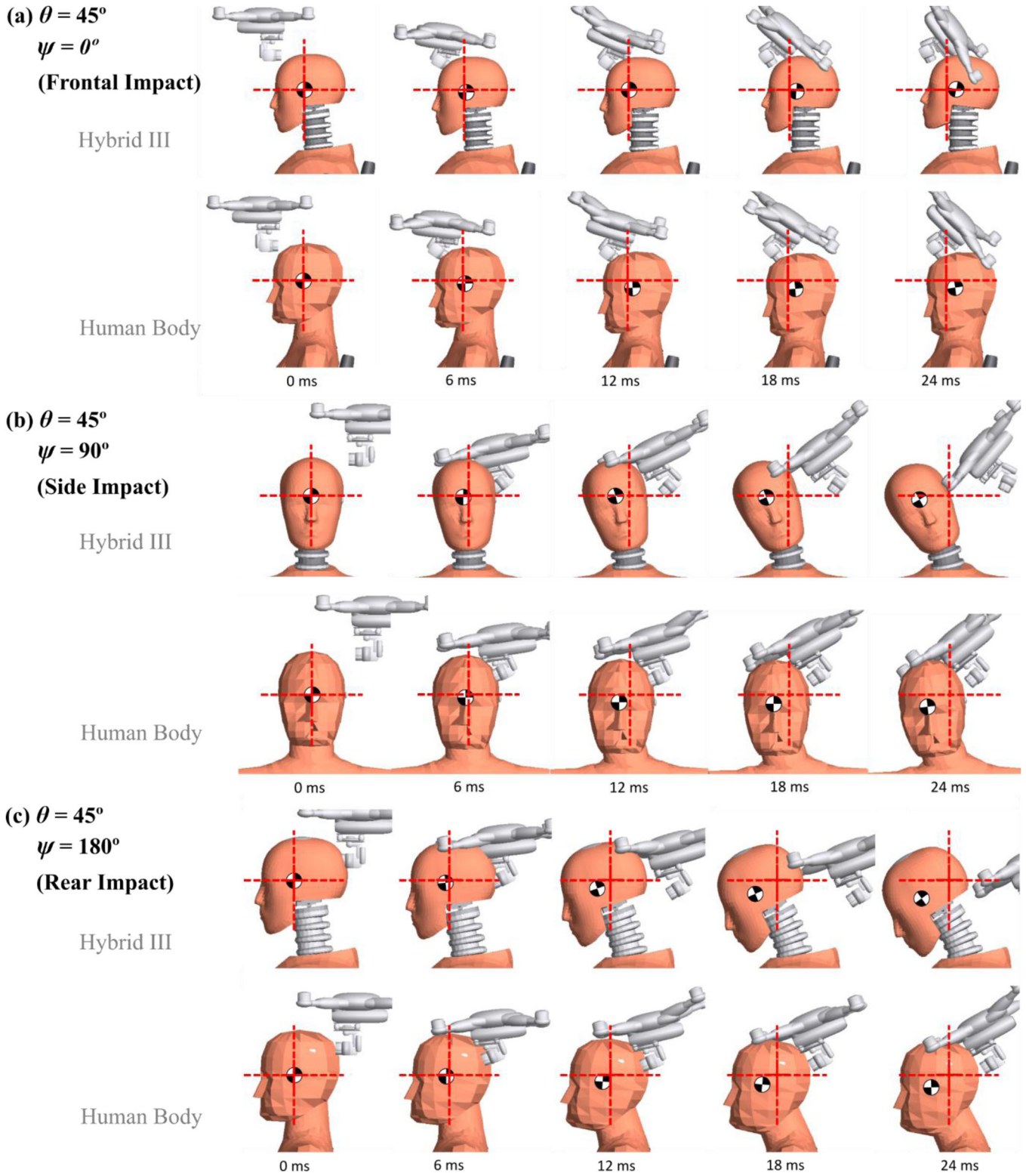
Figure 3. Comparison of impact sequences between the Hybrid III and the human body for $\theta = 0°$ (horizontal impact) at $\psi = 0°$, 90° and 180° at 196 J impact energy (equivalent to 18 m/s impact velocity).

displacements. The motion observed in this impact case is mostly head rotational motion head in an extension direction (backward) about the lower neck. Figure 3(b) shows a comparable head CG displacement between the Hybrid III and the human body. However, the head rotation about the body Z-axis is more significant in the human body in this case. For $\psi = 180°$ (rear impact) as shown in Figure 3(c), the Hybrid III head kinematics is comparable to the human body in which the neck section shows good bending curvature comparable to the human body neck.

Significant differences start to be observable when the impact elevation (θ) increases toward the vertical direction. Figure 4 shows the impact case of $\theta = 45°$ (elevated impact) of UAS hitting the heads from ψ of 0°, 90°, and

180°. In this case, where UAS impact elevation is at 45°, the downward deformation of the crash dummy neck is small when compared to the human body. The human body head rotational direction when ψ equal to 0°, 90°, and 180° is different from the Hybrid III. In Figure 4(a), for $\psi = 0°$ (frontal impact), the human body head rotates in flexion direction and vice versa in the Hybrid III. Also, in Figure 4(c) where the human body head rotates in extension direction but the Hybrid III rotates in flexion direction. Since the Hybrid III is designed primarily for frontal impact analysis, the head/neck construction holds anatomical difference compared to the human body head and neck construction which is more compliance in all load directions.

Figure 4. Comparison of impact sequences between the Hybrid III and the human body for $\theta = 45°$ (elevated impact) and $\psi = 0°$, $90°$ and $180°$ at 196 J impact energy (equivalent to 18 m/s impact velocity).

Lastly, the impact cases for $\theta = 90°$ (vertical drop) is shown in Figure 5. Even though the orientation of the UAS differs by $90°$ in each case, hitting locations are similar which results in similar head and neck kinematic in cases where ψ equals $0°$, $90°$, and $180°$. All three cases presented in Figure 5(a)–(c) show that the human body neck deforms more than the Hybrid III neck in a vertical direction. This shows an effect of

the stiff Hybrid III neck system compared to the human body neck system. Trajectory comparison shows the human head travels further down and over a longer period of time, while the Hybrid III head vertical displacement is small and with a faster rebound. In addition, the human head also rotates in extension direction when full vertical neck compression is reached, while such rotation is minimal in the Hybrid III head.
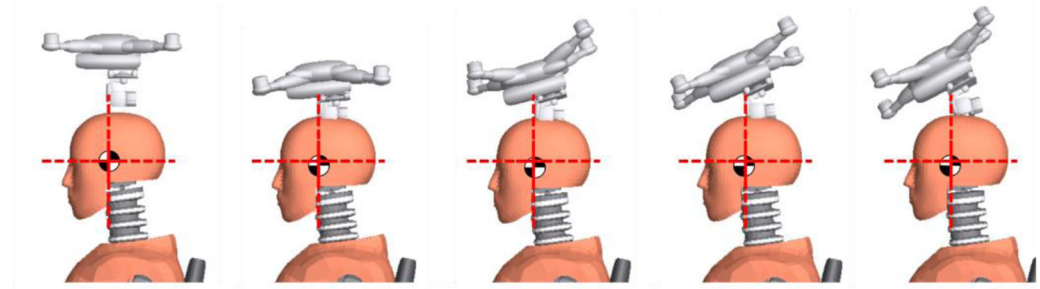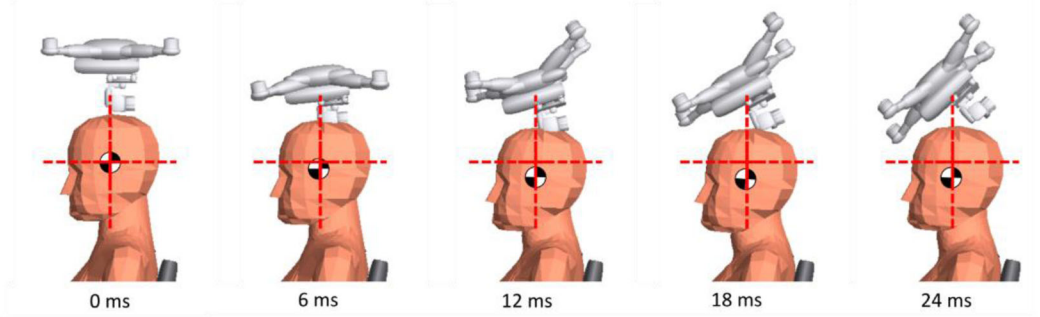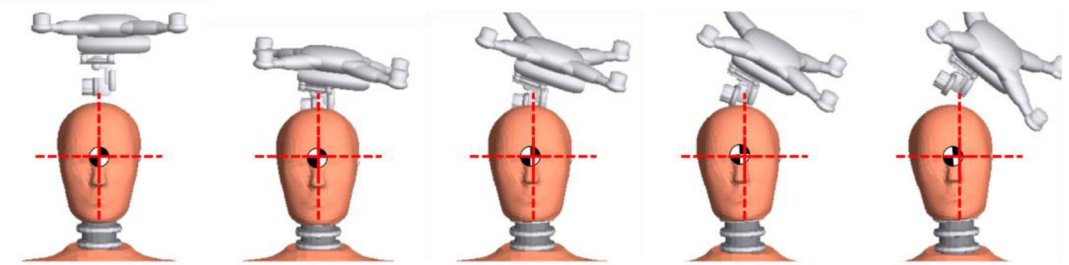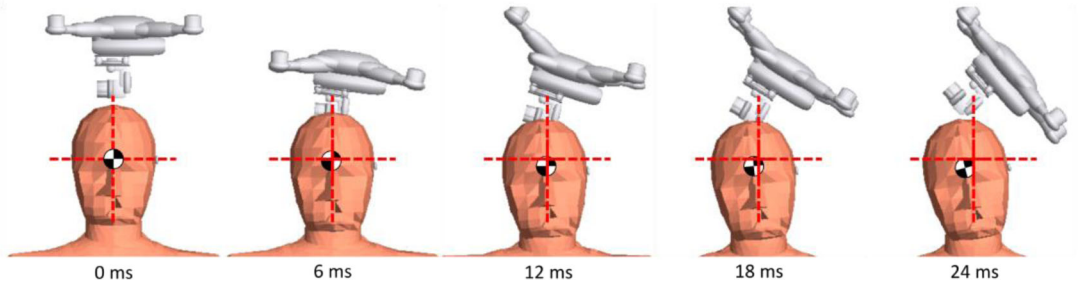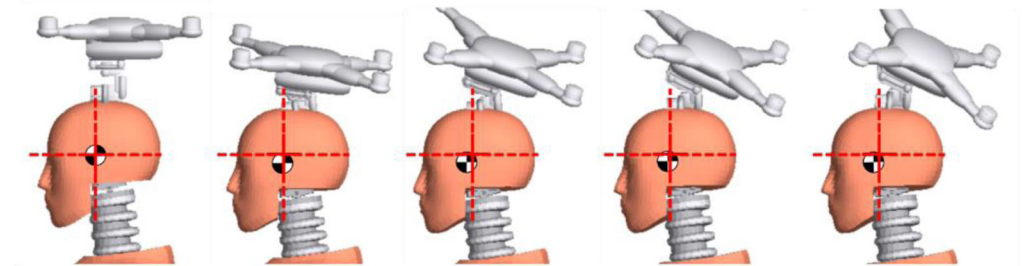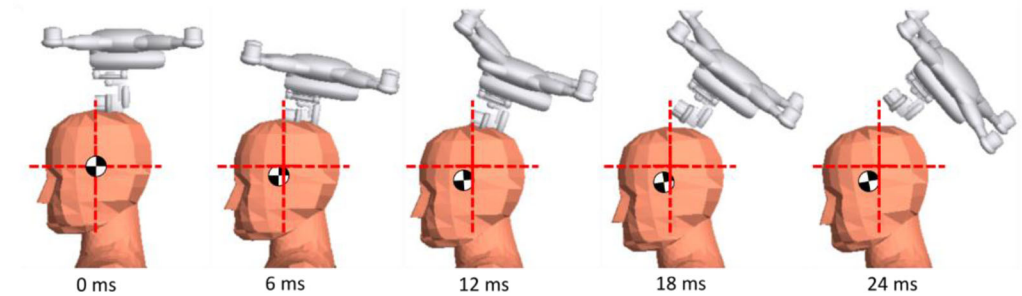
Figure 5. Comparison of impact sequences between the Hybrid III and the human body for $\theta = 90°$ (vertical drop) and $\psi = 0°$, 90° and 180° at 196 J impact energy (equivalent to 18 m/s impact velocity).

3.1.2. Head injury

Head injury criteria or HIC_{15} is an integral of head CG acceleration of a crash dummy or the human body heads. Before any difference in HIC_{15} can be realized, the difference in head CG acceleration between the Hybrid III and the human body has to be addressed. Appendix A shows a comparison of head CG acceleration between the Hybrid III and the human body models at various θ and ψ, and at 196 J impact energy (equivalent to an impact velocity of 18 m/s for the DJI Phantom III model).

As shown in Appendix A(a), for $\theta = 0°$ (horizontal impact), head CG acceleration signals produced from the Hybrid III and the human body models match well with one another, especially when $\psi = 0°$ (frontal impact). The phase of each signal also corresponds well between the model. However, the Hybrid III produces a higher acceleration peak than the human body when $\psi = 90°$ (side impact). For $\psi = 180°$ (rear impact), head CG acceleration matches well between the two models.

For impact cases where $\theta = 45°$ (elevated impact), significant differences in head CG acceleration can be observed as shown in Appendix A(b). For ψ of $0°$, $90°$, and $180°$, the first head CG acceleration peak which represents the contact force match well. Since both the Hybrid III and human skin share similar surface stiffness, these contact forces are similar in magnitude. The second peak, however, is higher for the human body compared to the Hybrid III for ψ of $0°$, $90°$, and $180°$. The second peak occurs when the entire UAS fully compresses and impact energy is fully transferred to the head. Overall, the area under the curves for the human body model is larger, showing the higher amount of impact energy being transferred to the head and results in higher head kinetic energy. In addition, the human body neck system damps out the impact force more than the Hybrid III since the observable third peak of the human body curve in Appendix A(b) dissipates out with a longer period.

Appendix A(c) shows impact cases when $\theta = 90°$ (vertical drop). Both models share similar trends with three observable peaks for $\psi = 0°$, $90°$, and $180°$. The phases of the first two peaks match well between the two models. Nevertheless, noted that the head CG of the human body accelerate faster as presented in the second peak. This shows that the human body neck complex is more compliant than the Hybrid III's. As for the rebound phase, the third peaks are 2.5 ms out of phase with one another. The last peak of the vertical impact case also shows a similar result to the elevated impact case where the neck of the human body rebound less and slower compared to the crash dummy. Furthermore, the differences in HIC_{15} between the two models tend to reach stable values as the energy increases beyond 100 J of impact energy.

By integrating the head CG acceleration-time history curve shows in Appendix A over the 15 ms time period, the HIC_{15} can be determined. Figure 6 shows a comparison of the HIC_{15} between the Hybrid III and the human body (upper plot) as well as the percentage difference of the HIC_{15} between the two models (lower plot). For every impact case in Figure 6, the HIC_{15} increases non-linearly as impact energy increases. The difference of the HIC_{15} between the two models vary differently for each impact case. The percentage plot shows a sharp drop from very low energy to approximately 20 J. This high percentage difference at very low impact energy can be neglected since the HIC_{15} values are near zero and have no practical injury significance.

For $\theta = 0°$ (horizontal impact) and $\psi = 0°$ (frontal impact), as shown in Figure 6(a), the Hybrid III produces similar results compared to the human body at with less than 7% difference at 196 J impact energy. For $\psi = 90°$ or $180°$ (side and rear impact), however, the human body produces higher HIC_{15} values compared to the Hybrid III by 23% and 47%, respectively at 196 J impact energy. This agrees with the head CG acceleration-time history in Figure 3 which shows larger head acceleration for the human body. Furthermore, the percentage differences for $\psi = 0°$, $90°$, and $180°$ reduce as the impact energy increases.

For θ equal to $45°$ (elevated impact), large discrepancies in HIC_{15} values can be observed in Figure 6(b). For $\psi = 0°$ (frontal) results in the smallest HIC_{15} difference of 53% at 196 J impact energy. Side ($\psi = 90°$) and rear ($\psi = 180°$) impacts, however, results in significantly large HIC_{15} differences of 75% and 77%, respectively. These findings confirm the impact sequences shown in Figures 3–5, which is observed that the amount of head displacement and the direction of head rotation differ between the Hybrid III and the human body. The Hybrid III head displacement is rather small and head rotation is in the opposite direction compared to the human body. This shows that more of the impact energy is transferred to the thorax through the stiff neck and results in less head acceleration for the Hybrid III. Furthermore, the percentage difference for $\psi = 0°$ and $\psi = 90°$ tend to reach stable values after the impact energy of 100 J at 50% and 80%, respectively. Impact case for $\psi = 180°$ also shows a tendency to reach a stable value of percentage difference, nevertheless, further analysis beyond 200 J is still required.

For $\theta = 90°$ (vertical impact), the HIC_{15} values for the Hybrid III and the human body are similar in all impact case ($\psi = 0°$, $90°$, and $180°$). The HIC_{15} percentage differences between the Hybrid III and the human body are approximately 33% for all three cases at 196 J impact energy. Since only impact direction (ψ) was varied, the UAS impact attitude and point of contact are similar in all three cases, only the facing direction of the UAS is changed by $90°$ in each case. The HIC_{15} percentage difference plot also shows the same trend for all three cases in vertical impact cases. The difference reduces as the impact energy increase, and the percentage difference reaches stable values at approximately 30% after 100 J impact energy.

Besides, it is observed in Figure 6 that HIC_{15} values are significantly higher at $\theta = 0°$ (horizontal impact) when compared to $\theta = 45°$ and $90°$. The explanation lies in the different points of contact between these impact cases. For $\theta = 0°$, UAS flies horizontally onto the head and has a front fuselage as the main point of contact. Other the other hand, for $\theta = 45°$ and $90°$, UAS collides onto the head with camera gimbal as the first point of contact. In comparison, front fuselage is considered to be structurally more rigid than the camera gimbal
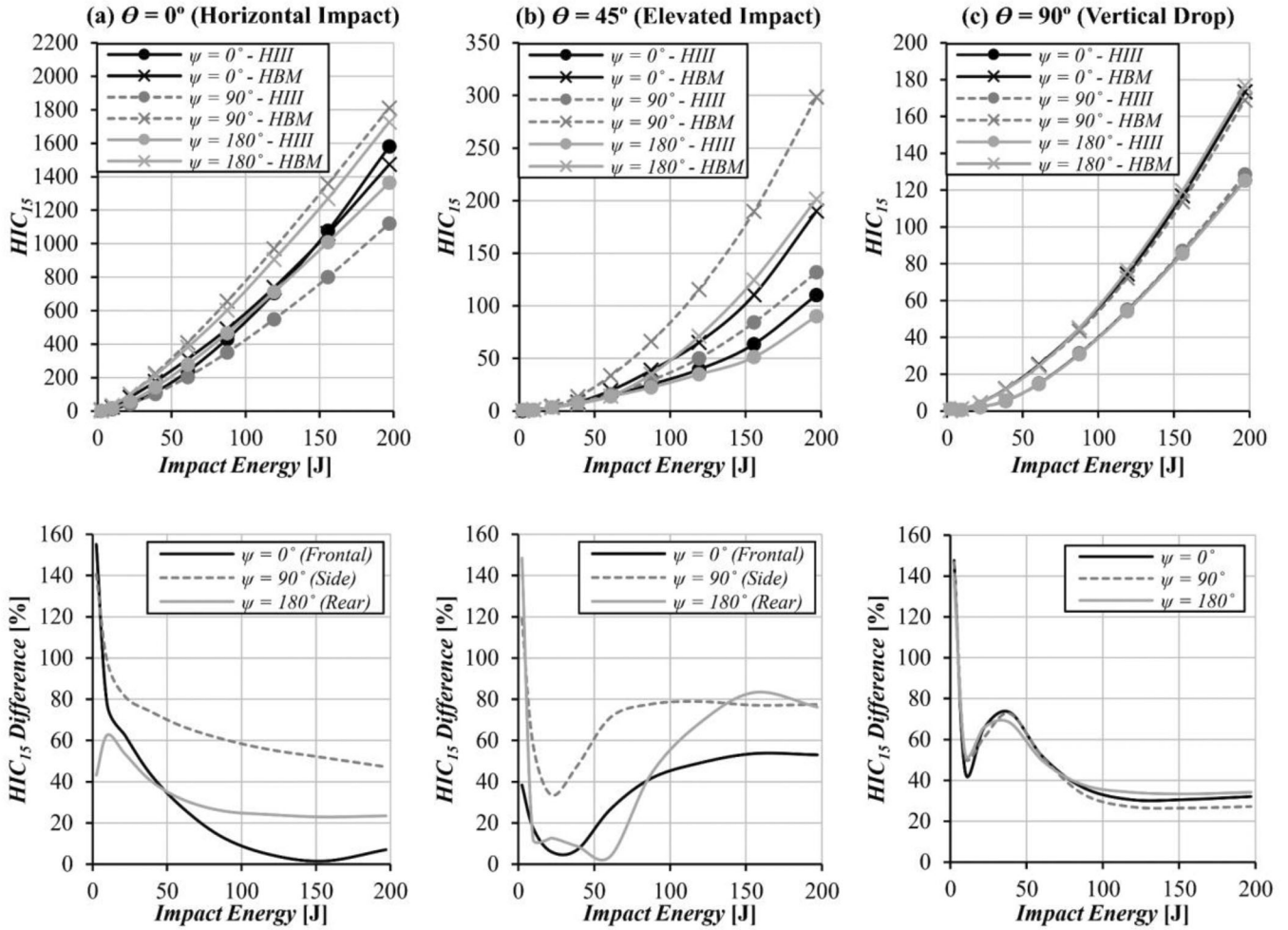
Figure 6. Comparison of HIC_{15} between the Hybrid III and the human body models (upper figures) and the percentage in HIC_{15} of Hybrid III dummy relative to the 100% for the human body (lower figures) at different impact energy, θ, and ψ.

which acts as a spring-damper system that damps out impact energy. This results in significantly lower impact energy transferred to the head when UAS drops vertically.

3.1.3. Neck injury

Neck responses between the Hybrid III and the human body are different due to the difference in neck biofidelic. In the Hybrid III, the neck complex is a segmented rubber and aluminum construction [23]. This results in the dummy neck to be less compliant compared to the human neck in a vertical direction. The difference can be seen in force/moment transferred to the neck system from the head. Appendix B and Appendix C show the difference in upper neck force in Z-direction ($F_{z,i}$) and upper neck moment about the Y-axis ($M_{Y,j}$) between the Hybrid III and the human body.

Upper neck force $F_{Z,i}$ produced by the Hybrid III peak upper neck force $F_{Z,i}$ is significantly higher than that in the human body. The area under the curve is smaller for the human body compared to the Hybrid III which shows that the amount of force transfers to the neck system over the first 16 ms period is much larger in the Hybrid III. The human body upper neck $F_{z,i}$ curve also shows a longer energy transfer period over time. In the model, the head of both the Hybrid III and the human body models are

modelled as a rigid sphere without any internal deformation such as the skull or brain deformation. This means that the force transfers from the head to the neck system in the Hybrid III are substantially higher than in the human body.

Furthermore, upper neck moment $M_{Y,j}$ in the dummy is significantly higher than the human body especially when $\theta = 0°$ (horizontal impact). Since the human body neck is made of small vertebrae, it allows more initial translational motion between inter-vertebral disc along the horizontal line before rotation when compared to the Hybrid III. The Hybrid III neck, on the other hand, is made of rubber and aluminium discs that allow rotation. This does not permit any translation between discs in the neck system. Therefore, the upper neck moment $M_{Y,j}$ of a Hybrid III is larger than the human body. Moreover, the rotational direction of the head affects the measured upper neck moment $M_{Y,j}$ in both magnitude and sign. It is shown in Appendix C that for $\psi = 0°$ and $180°$ impact cases, magnitude difference was observed but the measured moments all have the same sign. This is not the case when $\psi = 90°$ (side impact) and $\theta = 0°$, $45°$, and $90°$ (corresponding to horizontal, elevated, or vertical impact cases respectively). As clearly shown quantitatively in Figures 3(b), 4(b) and 5(b), the impact sequences illustrate the different head translational and rotational movements between the Hybrid III and the human body
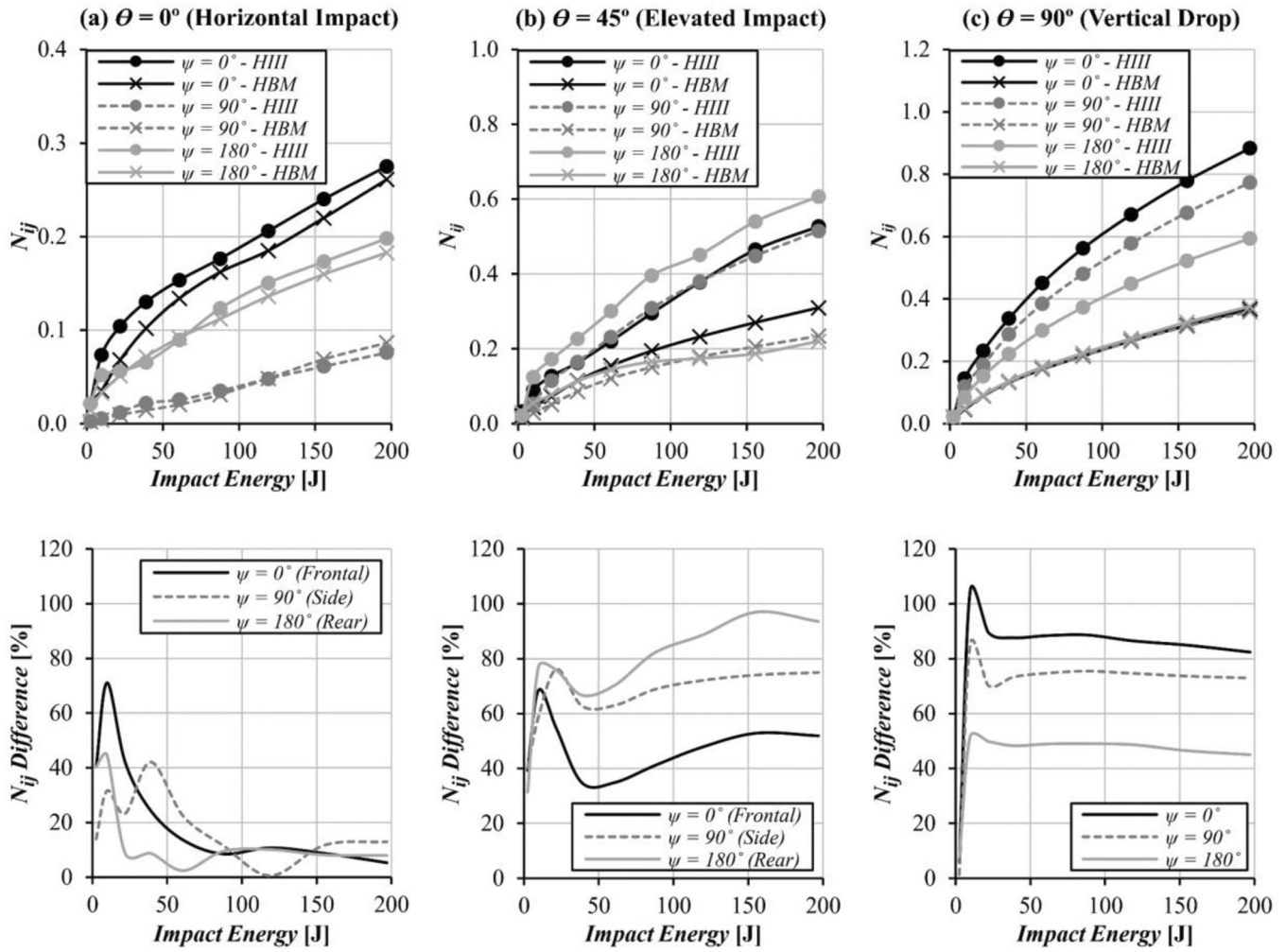
Figure 7. Comparison of N_{ij} between the Hybrid III and the human body models (upper figures) and the percentage in N_{ij} of Hybrid III dummy relative to the 100% for the human body (lower figures) at different impact energy, θ, and ψ.

models. This difference, however, is less severe for $\theta = 0°$ (horizontal impact).

A neck injury in the Hybrid III dummy and the human body is assessed using the neck injury criterion, N_{ij}, and the results are shown in Figure 7. N_{ij} criterion consists of four values, namely N_{TE}, N_{TF}, N_{CE}, and N_{CF}. The N_{ij} results presented here are the maximum of all four values combined for each different impact case. The impact case for $\theta = 0°$ (horizontal impact) shown in Figure 7(a) shows no significant difference between the Hybrid III and the human body for frontal, side, and rear impact cases. The percentage difference plot (lower figure of Figure 7(a)) also shows the 7% difference at 196 J impact energy for $\psi = 0°$, 90°, and 180° (corresponding to frontal, side, and rear impact cases, respectively). The peak percentage difference near 10 J impact energy can be neglected since the N_{ij} at that energy level has no significant neck injury level. In addition, the percentage difference starts to converge on a stable value of 7% percentage difference after 100 J of impact energy.

However, the differences become apparent for $\theta = 45°$ and 90° impact cases. For $\theta = 45°$ shown in Figure 7(b), the results for $\psi = 0°$ and $\psi = 90°$ are approximately 51% and 75% difference in the N_{ij} value at 196 J impact energy between the two models, respectively. For the impact case

with $\theta = 45°$ even a higher difference results between the N_{ij}'s for the Hybrid III and the human body: 93% difference at 196 J impact energy. To illustrate the effect of such difference in injury severity, in an elevated impact case with UAS approaching from the rear, the Hybrid III has 21% chance of broken neck while the human body has 14% chance of broken neck. This is based on the *AIS* injury level analysis, however, detail discussion of this injury level analysis is beyond the scope of this paper.

Similarly, for the impact cases of $\theta = 90°$ (vertical impact), the differences are 45%, 72% and 82% at 196 J impact energy at $\psi = 0°$, 90°, and 180°, respectively. Even though the upper neck force in Z-direction is comparable for $\psi = 0°$, 90°, and 180°, the neck moments vary between these cases due to a slight shift in impact location of the UAS on the head. This results in a change in induced upper neck moment M_Y. This shows that neck moment has a significant impact on the neck injury.

4. Discussion

The previous Section assessed differences in injury levels of the Hybrid III dummy relative to the human body due to various DJI Phantom III UAS collisions. To accomplish this

validated multibody system (MBS) models of DJI Phantom III UAS collisions with a Hybrid III dummy and with a human body have been implemented in MADYMO[11]. The MBS modelling technique allows fast simulation time with accurate results and can capture accurately the overall kinematics of the system. By varying impact elevation (θ) and impact direction (ψ), a total of 9 impact cases were simulated in the previous Section both for MBS models of human body and Hybrid III dummy. Table 1 summarizes the results obtained for these 9 impact cases in terms of head/neck injury differences of the Hybrid III dummy relative to the human body.

Table 1 shows that, for horizontal impact with UAS approaching from the front (impact case 1) and rear (impact case 3), the dummy produces similar response and similar head/neck injuries as the human body. For horizontal UAS impact from side direction (impact case 2), the Hybrid III predicts similar neck injury, but higher head injury than the human body.

Table 1 also shows that for the other impact cases 4 through 9 (i.e. 45 degree elevated and vertical drop) the Hybrid III under-predicts head injury and over-predicts neck injury relative to the human body.

To understand these systematic differences, the MBS models of the Hybrid III and the human body were compared anatomically. These MBS models differ for the neck, though they are almost identical for the head. The heads of both MBS models are represented by a rigid body with the same contact force model and without any internal deformation. This means that the differences in head and neck injuries found in Section 3 stem from the differences in neck complexes of the two models which affect neck deformation and resistance to head acceleration.

The neck system in the Hybrid III dummy is constructed by a straight column in which a higher impact force from the head is transferred to when compared to the human head. The more compliance human body neck system is modelled realistically to represent the vertebrae structure with passive muscle force. This allows the head to travel faster in a downward direction with less resisting upward force, resulting in larger head acceleration and lower neck force. As shown in the qualitative analysis of the impact sequences in Figures 3–5, head displacement and neck deformation in the human body is larger than the Hybrid III. A lack of biofidelity in the Hybrid III neck is attributed to high resistance to compressive force and bending of the neck and torso [6], leading to the tendency to over-estimate axial compressive force. This is confirmed by the neck injury analysis using the N_{ij} criterion which shows the Hybrid III over-predicts N_{ij} values compared to the human body.

It should be noted that the human neck stiffness and load-bearing characteristics change dramatically when spinal curvature is included [24]. Such curvature shifts the load path of the centre of the thoracic spine by more than 1 cm, resulting in less force transferred directly towards the thorax. Without neck curvature under vertical load condition, the Hybrid III neck becomes stiffer than the human spine, and load is transferred more directly to the thorax. In addition, with small vertebrae in the human body,

translational motion between inter-vertebral disc is possible and allow neck compliance in all direction. The effect of this can be seen in elevated impact (impact cases 4, 5, and 6) where the human body head has a combination of both rotational and translational motions. A related effect is found when the UAS flies horizontally and approaches the head from the side (impact case 2). The head translational motions are different as well as the direction of head rotation about the Z-axis. This results in the estimation of neck moments to have an opposite sign between the two models.

5. Conclusions

When conducting an impact testing research, it is important to account for the type of crash dummy used and recognize the accuracy limitation relative to a real human body. To better understand this difference, this paper investigates the differences in head and neck injury levels between a 50th percentile Hybrid III crash dummy and a 50th percentile human body subjected to UAS collisions. To simulate such collision, a validated UAS MBS model was employed in impact simulation against validated Hybrid III dummy and human body models in MADYMO. For the UAS, the DJI Phantom III was chosen as a representative model used in this study. A total of 9 impact cases were investigated which include horizontal, elevated, and vertical impacts, as well as impact directions from the front, side, and rear relative to the head.

The simulation results show that for horizontal UAS approaches from front and rear, Hybrid III head and neck injuries are similar relative to those for the human body. However, when UAS approaches horizontally from side direction, then head acceleration is higher for Hybrid III. Furthermore, when UAS drops vertically or impacts under 45 degrees elevation, then Hybrid III predicts lower head injury and higher neck injury for each impact direction, i.e. frontal, side and rear.

Differences in head and neck injuries are due to the difference in the neck complex between the two models. Hybrid III has a stiffer neck complex when compared to the human body, which limits Hybrid III's head movements, especially in the vertical direction. This implies smaller head acceleration for the Hybrid III head and instead a larger amount of impact energy is transferred through the Hybrid III neck to the thorax. In contrast to this, the human neck is much more compliant because it consists of a complex of small vertebrae which allows a larger neck deformation. Hence, the human neck experiences lower force and moment, while the head experiences larger head acceleration.

From a UAS impact severity analysis perspective, the Hybrid III dummy has a realistic response relative to the human body especially for horizontal impacts from frontal or rear directions. This finding reaffirms other works that show that the focus of the Hybrid III design and validation has been on a horizontal-frontal load direction [25,26]. Nevertheless the Hybrid III dummy has serious limitations for horizontal UAS impact from side direction and vertical UAS drops as well as elevated UAS impacts. This limitation of the Hybrid III dummy does not apply to the MBS model

of the human body. The latter has been validated against real human and cadavers, making it possible to realistically simulate various impact cases in all load directions. This is an important benefit of using the numerical human body model with multi-directional biofidelity [15].

The results obtained also reveal novel insight into how different impact conditions can significantly affect injury levels. A slight change in impact elevation may change the point of contact which can result in a completely different injury level. To extend the analysis to cover larger scenarios, other parameters need to be incorporated and investigated in future works, for example, off-set between UAS CG and head CG, UAS initial rotational velocity, or yaw and roll angles. More importantly, the variation of mass, size, and shape of UAS, which are influential parameters on injury severity, will also be investigated in future works.

Disclosure statement

No potential conflict of interest was reported by the author(s).

ORCID

Borrdephong Rattanagraikanakorn (iD) http://orcid.org/0000-0002-1489-8777
Riender Happee (iD) http://orcid.org/0000-0001-5878-3472

References

[1] Campolettano ET, Bland ML, Gellner RA, et al. Ranges of Injury Risk Associated with Impact from Unmanned Aircraft Systems. Ann Biomed Eng. 2017;45(12):2733–2741. http://link.springer.com/10.1007/s10439-017-1921-6.

[2] Arterburn DR, Duling CT, Goli NR. Ground Collision Severity Standards for UAS Operating in the National Airspace System (NAS). 17th AIAA Aviation Technology, Integration, and Operations Conference; 2017. p. 1–16, https://arc.aiaa.org/doi/10.2514/6.2017-3778.

[3] Arterburn D, Ewing M, Prabhu R, et al. FAA UAS Center of Excellence Task A4 : UAS Ground Collision Severity Evaluation, Huntsville; 2017. http://www.assureuas.org/projects/deliverables/a4/ASSURE_A4_Final_Report_UAS_Ground_Collision_Severity_Evaluation.pdf.

[4] Huculak R, NIAR UAS Drop Testing Report, Wichita; 2016. http://www.assureuas.org/projects/deliverables/a11/NIAR. Test Report - FAA-UAH UAS Drop Testing.pdf.

[5] Mroz K, Bostrom O, Bengt P, et al. Comparison of Hybrid III and human body models in evaluating thoracic response for various seat belt and airbag loading conditions. IRCOBI Conference, Sept 15-16; 2010. p. 265–280.

[6] Herbst B, Forrest S, Chng D, et al. Fidelity of anthropometric test dummy necks in rollover accidents, https://www-nrd.nhtsa.dot.gov/pdf/esv/esv16/98s9w20.pdf%0A.

[7] Sances A, Kumaresan S. Comparison of biomechanical head-neck responses of hybrid III dummy and whole body cadaver during inverted drops. Biomed Sci Instrum. 2001;37:423–427. http://www.ncbi.nlm.nih.gov/pubmed/11347428.

[8] Sances A, Carlin F, Kumaresan S. Biomechanical analysis of head-neck force in hybrid III dummy during inverted vertical drops. Biomed Sci Instrum. 2002;38:459–464. http://www.ncbi.nlm.nih.gov/pubmed/12085650.

[9] Rattanagraikanakorn B, Schuurman MJ, Gransden DI, et al. Modelling Head Injury due to Unmanned Aircraft Systems Collision: Crash Dummy vs Human Body. AIAA Aviation 2019 Forum, Dallas, Texas; 2019. https://arc.aiaa.org/doi/abs/10.2514/6.2019-2835.

[10] TASS International, MADYMO; 2019. https://tass.plm.automation.siemens.com/madymo.

[11] Rattanagraikanakorn B, Gransden DI, Schuurman M, et al. Multibody system modelling of unmanned aircraft system collisions with the human head. Int J Crashworthiness. 2019; 1–19. DOI: 10.1080/13588265.2019.1633818

[12] Manning JE, Happee R. Validation of the MADYMO Hybrid II and Hybrid in Vertical Impacts III 50th-Percentile Models. Test. 1998. p. 26–28.

[13] TASS International, Model Manual Version 7.7; 2017.

[14] Happee R, Hoofman M, Van Den Kroonenberg AJ, et al. A Mathematical Human Body Model for Frontal and Rearward Seated Automotive Impact Loading, SAE Technical paper; 1998.

[15] Happee R, Ridella S. Mathematical human body models representing a mid size male and a small female for frontal, lateral and rearward impact loading. IRCOBI Conference Proceedings; 2000. pp. 1–18,

[16] TASS International, Human Body Models Manual Version 7.7; 2017.

[17] Hardy W, Khalil T, King A. Literature review of head injury biomechanics. Int J Impact Eng. 1994;15(4):561–586.

[18] Henn HW. Crash tests and the head injury criterion. Teach Math Appl. 1998;17(4):162–170.

[19] Hutchinson J, Kaiser MJ, Lankarani M. The Head Injury Criterion (HIC) functional. Journal of Applied Mathematics and Computation. 1998;96(1):1–16.

[20] Schmitt K-U, Niederer PF, Muser MH, et al. Head Injuries. Trauma Biomechanics. Berlin, Heidelberg: Springer; 2010. pp. 63–93. http://link.springer.com/10.1007/978-3-642-03713-9_3.

[21] Klinich K, Saul R, Auguste G, et al. Techniques for Developing Child Dummy Protection Reference Values; 1996.

[22] Parr MJC, Miller ME, Bridges NR, et al. Evaluation of the Nij neck injury criteria with human response data for use in future research on helmet mounted display mass properties. Proceedings of the Human Factors and Ergonomics Society; 2012. p. 2070–2074,

[23] Humanetics, Hybrid III 50th Male. http://www.humaneticsatd.com/crash-test-dummies/frontal-impact/hiii-50m.

[24] Herbst B, Forrest S, Chng D, et al. Fidelity of Anthropometric Test Dummy Necks in Rollover Accidents; 1382. p. 14–15.

[25] Taylor A. Comparison of the Hybrid II, FAA Hybrid III, and THOR-NT in Vertical Impacts; 2016. https://outlook.office.com/owa/?path=/attachmentlightbox.

[26] Arosio B, Mongiardini M, Mattos GA, et al. Comparison of hybrid III and human body model in head injury encountered in pendulum impact and inverted drop tests. First International Roadside Safety Conference; 2017.

Appendix A – head CG acceleration-time history
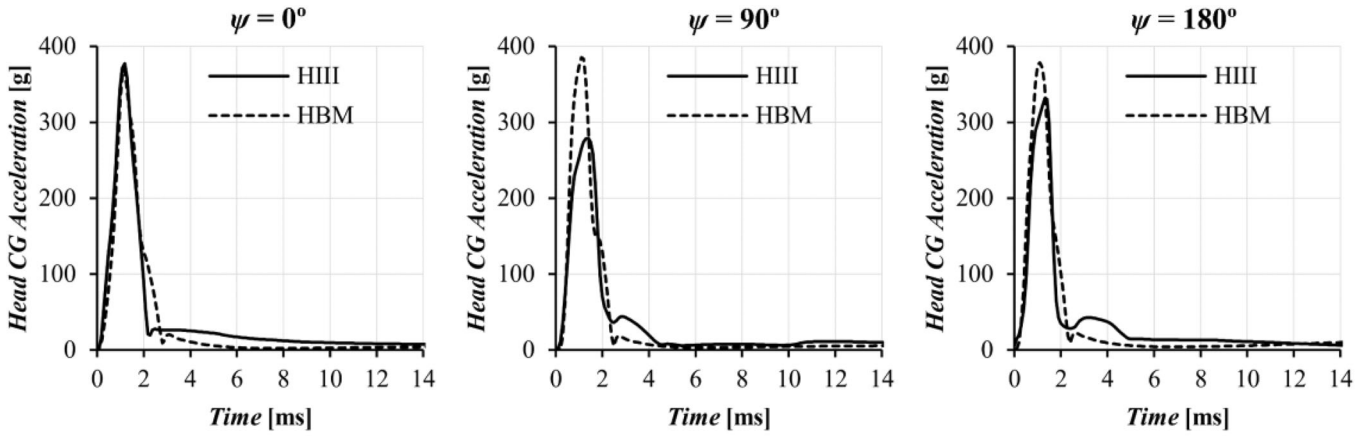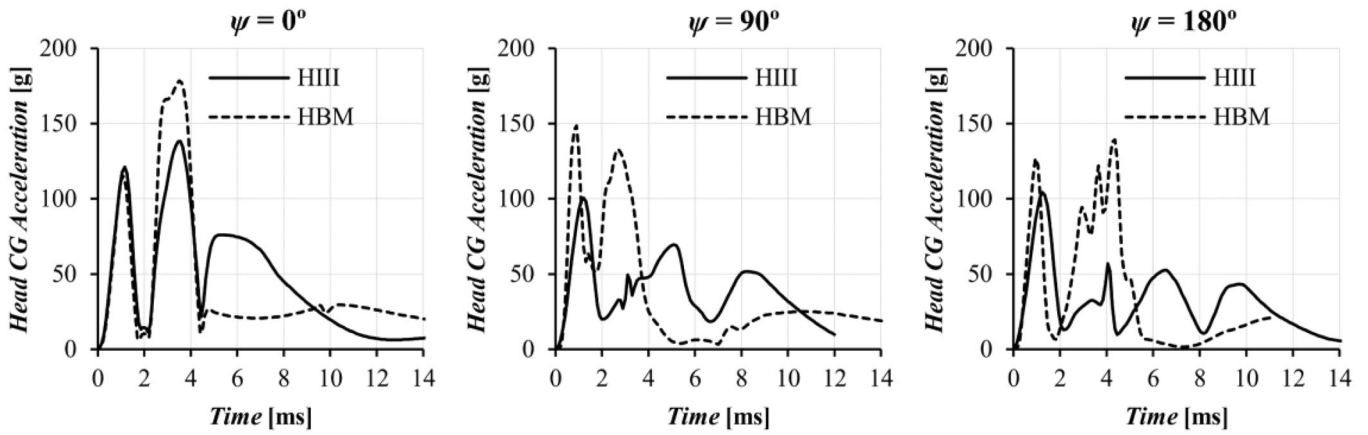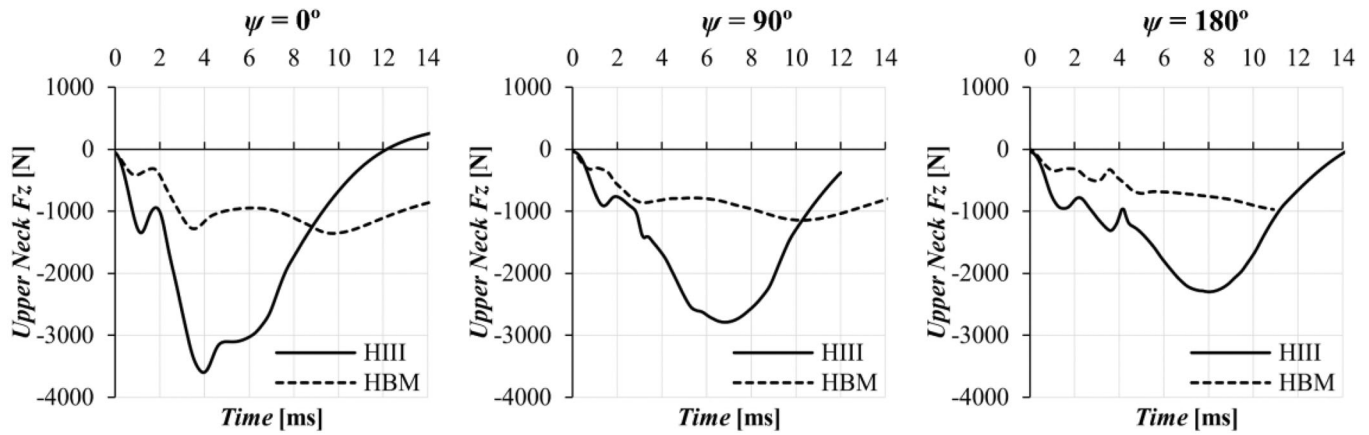
(a) $\theta = 0°$
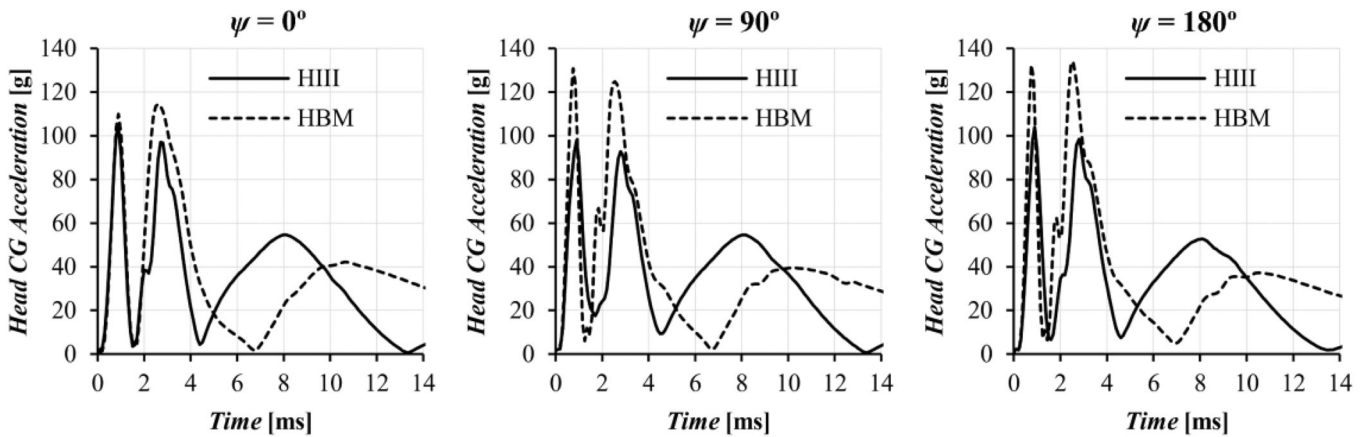
Comparison of head CG acceleration between the Hybrid III and the human body models at various impact conditions and at 196 J impact energy (equivalent to 18 m/s impact velocity)
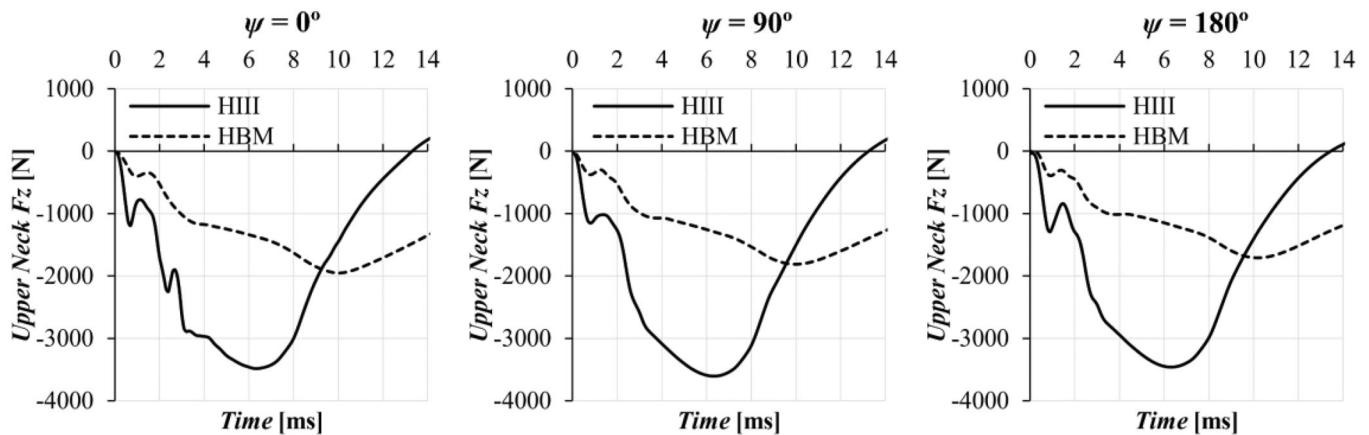
Appendix B – upper neck F_z-time history

(a) $\theta = 0^\circ$
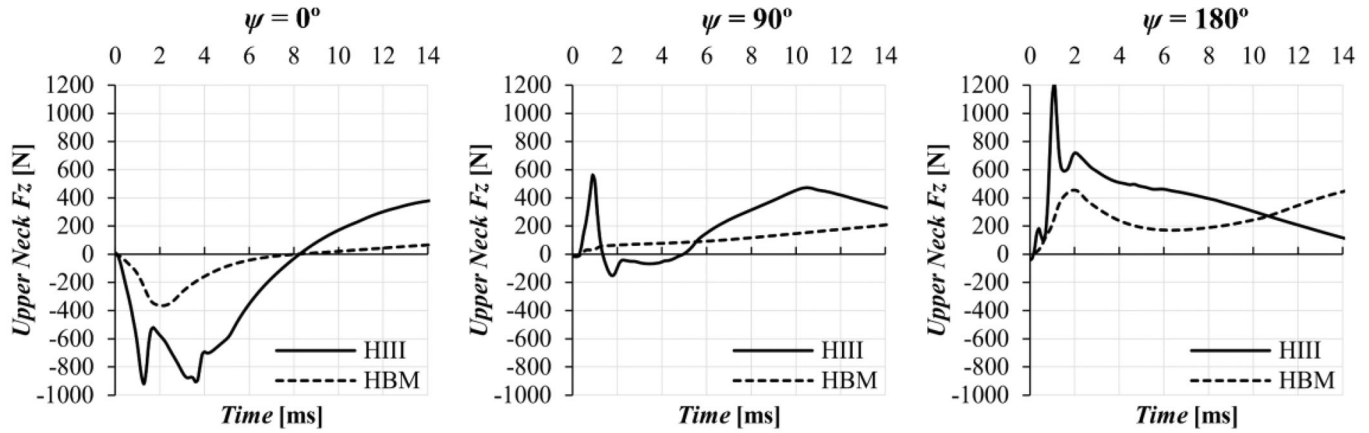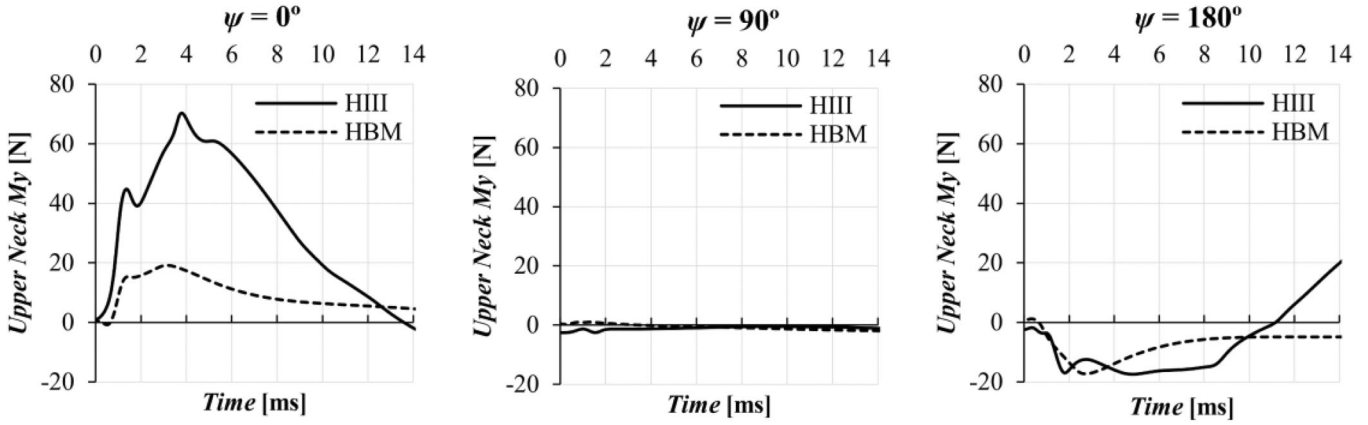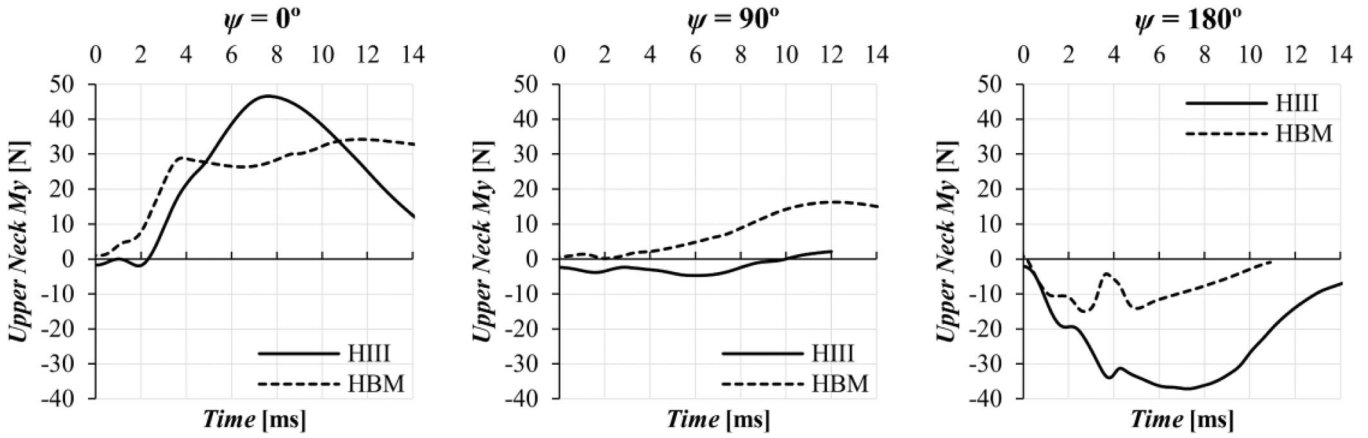

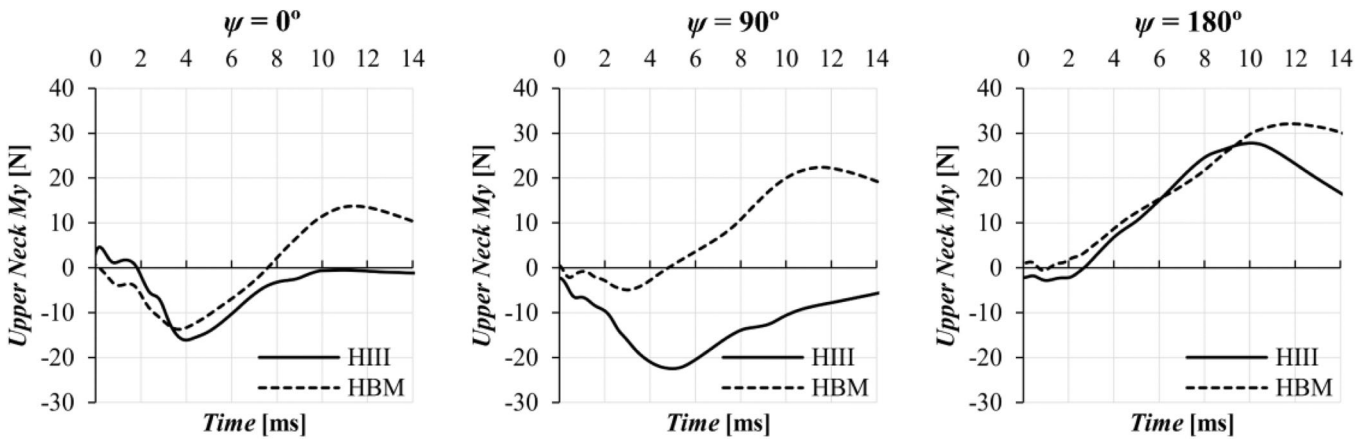### (b) $\theta = 45^\circ$

(c) $\theta = 90^\circ$

Comparison of upper neck force in Z-direction between the Hybrid III and the human body models at various impact conditions and at 196 J impact energy (equivalent to 18 m/s impact velocity)

Appendix C – upper neck M_Y-time history

(a) $\boldsymbol{\theta = 0^o}$

(b) $\boldsymbol{\theta = 45^o}$

(c) $\boldsymbol{\theta = 90^o}$

Comparison of upper neck moment about Y-axis between the Hybrid III and the human body models at various impact conditions and at 196 J impact energy (equivalent to 18 m/s impact velocity)